Computational Fluid Dynamics to Evaluate the Management of a Giant Internal Carotid Artery Aneurysm

Jonathan Russin[1], Haithem Babiker[2], Justin Ryan[2], Leonardo Rangel-Castilla[1], David Frakes[2], Peter Nakaji[1]

Key words
- Cerebrovascular
- Computational fluid dynamics
- Giant cerebral aneurysm
- Extracranial/intracranial bypass
- Flow modeling
- Wall shear stress

Abbreviations and Acronyms
ACA: Anterior cerebral artery
BTO: Balloon test occlusion
CFD: Computational fluid dynamics
CT: computed tomography
ICA: Internal carotid artery
MCA: Middle cerebral artery
WSS: Wall shear stress

From the [1]Department of Neurological Surgery, University of Southern California, Los Angeles, California, USA; and [2]School of Biological and Health Systems Engineering, Arizona State University, Tempe, Arizona, USA

To whom correspondence should be addressed: Jonathan Russin, M.D. [E-mail: jonathan.russin@med.usc.edu]

Citation: World Neurosurg. (2015) 83, 6:1057-1065. http://dx.doi.org/10.1016/j.wneu.2014.12.038

Journal homepage: www.WORLDNEUROSURGERY.org

Available online: www.sciencedirect.com

■ BACKGROUND: **Giant intracranial aneurysms are rare lesions that present uniquely complex therapeutic challenges. Computational fluid dynamics (CFD) has been used to simulate the hemodynamic environments of developing and ruptured cerebral aneurysms. In this study, we use CFD to examine retrospectively hemodynamic changes during the complicated clinical course of a giant carotid aneurysm.**

■ OBJECTIVE: **To take an innovative, CFD-based approach to retrospective analysis of the surgical management and clinical course of a giant carotid aneurysm.**

■ METHODS: **Pre- and posttreatment image data were first segmented to produce computational aneurysm models. Flow within the models was then simulated using CFD. Simulated flow and wall shear stress (WSS) profiles were analyzed and used to examine hemodynamic changes during the clinical course of the patient, after 2 independent treatments.**

■ RESULTS: **Greater WSS magnitudes and a more localized flow impingement region were observed at the distal portion of the aneurysm after both clinical interventions. These relative, acute changes in hemodynamic features at the distal aneurysm wall were greatest after the second intervention and may have preceded rupture of the aneurysm in that region.**

■ CONCLUSIONS: **The application of CFD to the management of a giant intracranial aneurysm showed unexpected posttreatment changes in flow and WSS profiles. The simulation results offer a viable explanation for the observed clinical course. This study demonstrates potential for the use of CFD preoperatively for decision-making in the surgical and endovascular management of intracranial aneurysms.**

INTRODUCTION

Giant intracranial aneurysms are relatively rare, representing less than 5% of all cerebral aneurysms (20); however, these complex lesions are associated with a much greater risk of rupture than smaller aneurysms and pose unique treatment challenges (15, 20). Computational fluid dynamics (CFD) has been used previously to explore the biomechanical mechanisms that precipitate aneurysm formation and rupture (12, 13, 17). Nevertheless, previous studies have focused largely on the chronic effects of wall shear stress (WSS) on the integrity of the vessel wall. Furthermore, no previous study has applied CFD to retrospectively examine serial hemodynamic changes during the complex combined surgical and endovascular management of a giant cerebral aneurysm. This current analysis focuses on the acute changes in flow and WSS after successive interventions in an attempt to explain the clinical outcome. We first present the patient's case and the CFD methods. Simulated results are then presented and discussed in relation to the clinical course of the patient.

CASE PRESENTATION

A 44-year-old, right-handed white woman presented to our institution complaining of progressive visual loss during the past year. The patient reported that her symptoms were more severe in the left eye. She denied any severe headaches, nausea/vomiting, weakness in extremities, or any other neurologic symptoms. On examination, we found she was neurologically intact except for vision. In the left eye the patient could not reliably perceive light, had a pale optic disc, and had an afferent pupillary defect. A noncontrast computed tomography (CT) scan of the head was obtained in the emergency department, and findings prompted a CT angiogram of the brain that confirmed the diagnosis of a giant fusiform left carotid artery aneurysm (**Figure 1**). A 4-vessel cerebral angiogram was performed along with a balloon test occlusion (BTO) of the left internal carotid artery (ICA) (**Figure 2**). A bypass procedure to augment cerebral blood flow was considered; however, on the basis of the

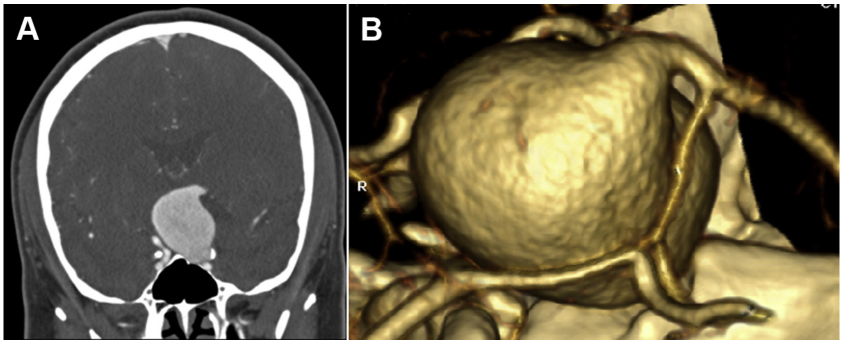

Figure 1. (**A**) Coronal computed tomography angiogram showing a giant left internal carotid artery aneurysm. (**B**) A 3-dimensional reconstruction of the same aneurysm with a view across the planum and over the contralateral A1 segment.

patient's asymptomatic response to the BTO, it was deferred initially. The patient tolerated the BTO, and the left ICA was occluded just proximal to the petrous segment.

Immediately after the procedure, the patient had acute onset of aphasia and right hemiplegia that lasted approximately 10 minutes and was treated with pressors and fluids. Repeat imaging showed no hemorrhage or evidence of infarct, and findings of the patient's examination returned to baseline. After 5 days in the hospital, the patient had been weaned off of pressors and was scheduled for discharge when she developed right-sided weakness again. An emergency CT scan of the head was obtained and was significant for a hypodensity in the left posterior frontal region (Figure 3). A CT perfusion study was obtained and was significant for increased mean transit time and decreased flow with relatively preserved cerebral blood volume (Figure 4).

On the basis of the patient's clinical symptoms, we decided to perform a superficial temporal artery to MCA bypass. The anastomosis was performed to a cortical branch in the posterior Sylvian fissure. The patient tolerated the procedure well and postoperative angiography showed that the bypass was perfusing the ipsilateral middle cerebral artery (MCA) and proximal anterior cerebral artery (ACA) up to the anterior communicating artery (Figure 5). On postoperative day 2, the patient had acute onset of headache, nausea, and vomiting, and an emergency CT of the head was significant for acute subarachnoid hemorrhage (Figure 6). The residual aneurysm present at the time of rupture is modeled in Figure 7C. The majority of the hemorrhage in the subarachnoid space was localized to the posterior superior region of the aneurysm (Figure 6). The patient required an emergency ventriculostomy and was monitored in the intensive care unit for the next 14 days. At the time of discharge, the patient had persistent right-sided weakness and required full time care.

Figure 3. Noncontrast computed tomography of the head that is significant for a hypodensity in the posterior left frontal lobe anterior cerebral artery/middle cerebral artery watershed region (*arrow*).

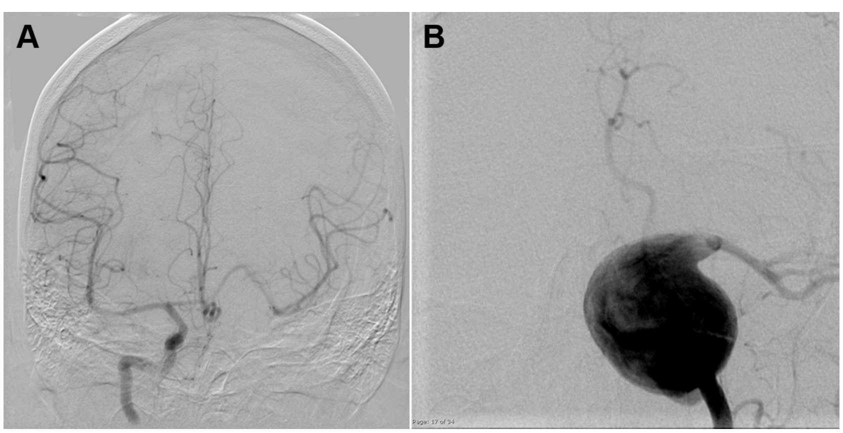

Figure 2. (**A**) Cross compression anteroposterior angiogram showing almost simultaneous filling of the contralateral middle cerebral artery tree. (**B**) Left internal carotid artery injection showing the giant fusiform left ICA aneurysm.

SIMULATION METHODS

To evaluate the posttreatment hemodynamics within the aneurysm, CT image data were used to reconstruct the pre-treatment, post-ICA occlusion, and post-bypass aneurysmal geometries. The image data were first segmented with Mimics software (Materialize, Leuven, Belgium) to form 3-dimensional computational models of the aneurysm and associated vessels. In all the examined cases, the inflow branch was segmented up to the next upstream bifurcation, which ensured that the longest possible length of the inflow branch without bifurcation was modeled, thereby enabling meaningful CFD simulations (16). Inflow branch lengths were greater than 15X, 7X, and 6.5X the mean